deformations occurring during the FB hole flanging process were predicted by the finite element method. The FEM simulation results were compared with experimental results and were found to be in strong agreement with each other. The results of this study verify that FB hole flanging process resulted is better flange shapes and flangeability than those obtained by the conventional hole flanging process. In 2007, Mueller *et al.* [6] demonstrated severe plastic deformation of magnesium alloy AZ31. They utilized two methods to modify the extrusion process and control the yield point under compressive loading, which was significantly lower than that under tensile loading. In 2007, Liu *et al.* [7] used experimental and simulated extrusion of magnesium alloy AZ31 into a rectangular section at different ram speeds. In 2008, Tsai *et al.* [8] investigated the stamping process for manufacturing a notebook top cover case with LZ91 magnesium-lithium alloy sheet at room temperature was examined using both the experimental approach and the finite element analysis. In order to validate the finite element analysis, an actual four-operation stamping process was conducted with the used of 0.6mm thick LZ91 sheet as the blank. A good agreement in the thickness distribution at various locations between the experimental data and the finite element results confirmed the accuracy and efficiency of the finite element analysis. The superior formability of LZ91 sheet at room temperature was also demonstrated in the present study by successful manufacturing of the notebook top cover case.

II. EXPERIMENTAL METHODS AND PROCEDURES

In order to find the stress-strain relationship of fabrication material, the equipment for the compression experiment of billet used by the study is China Steel Corporation's tester for all high-speed metal forming tester. And the device for the forging experiment of bearing cover parts is a 4000 kN hydraulic press, with its appearance shown in Fig. 1. First of all, a compression test is made to AZ31 magnesium alloy cylindrical specimens. The specifications of the specimens are based on the ASTM standard, with diameter 6mm and height 9 mm to perform the compression test. As for the forging experiment of bearing cover parts, the rods with diameter 30mm and heights 85mm and 80mm are used to perform the experiment. The experimental temperature of specimen is at the range 280°C ~ 350°C, under which forming can be undergone smoothly. However, when the temperature exceeds 450°C, under the condition of no protection gas, the compressed magnesium alloy shatters and becomes powder.

Fig. 1 4000 kN hydraulic press.

AZ31 magnesium alloy cylindrical specimens are carried out compression tests under different temperatures and different strain rates. The heights of the compressed specimens are measured, and the compression load is retrieved by computer. After that, a stress-strain curve can be drawn, with the result shown in Fig. 2. The experimental results under identical conditions demonstrated that with a relationship between ram speeds and forming load established, extrusion temperature at different ram speeds could be predicted easily. This study conducts experiments and uses the DEFORM 3D program for simulations under different temperatures, and then analyzes investigation on the formability of magnesium alloy of 3C products under hybrid embossing process. Via investigation results, fabrication conditions can be identified that decrease the incidence of cracking and insufficient filling of finished products.

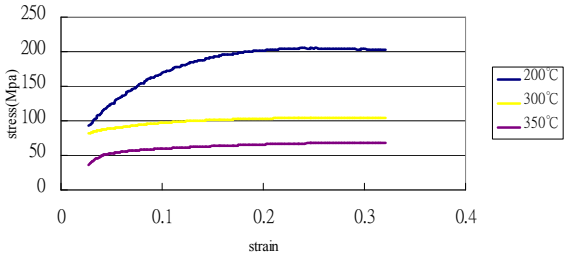

(a) Strain rate=0.05/s

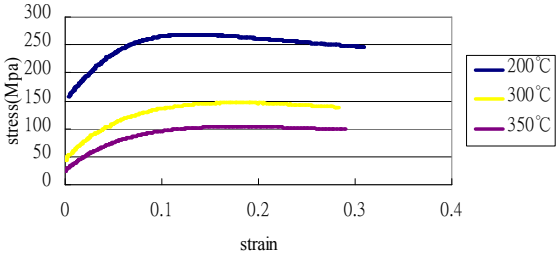

(b) Strain rate=3/s

Fig. 2 Stress-strain curve of the AZ31 magnesium alloy.

III. Results and discussion

Through embossing process, billets are able to achieve the target dimensions that finished products require, as shown in Fig. 3. As forming begins, action force is given around a sheet, producing plastic deformation of the sheet and bending it gradually. When the punch distance increases continuously, embossing patterns are gradually formed at the central part of the sheet, and spill edge also starts forming. When the stroke reaches 7.4 mm, the height of the embossing part reaches the position with a preset height 1 mm. During this time, the space of cavities is fully filled with material, with excessive material moving to the two sides of the cavities, and thus forming the spill edge. Then the filling of cavities is completed, and its load tends to rise rapidly. The relationship between temperature and load

when forming under different temperatures is shown in Fig. 4.

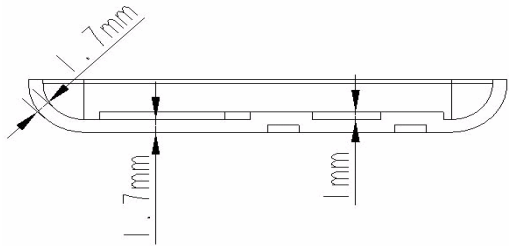

Fig. 3 Dimensions of finished products under embossing process

The paper explores the effects of different billet thicknesses on the formability of sheets under embossing process. The billets adopted for simulation is preset to be of thickness 2.1 mm, 2.4 mm and 2.7 mm respectively. The billets of 3 different thicknesses can meet the required forming height of the embossing style. As seen from the comparison between forming situation and sheet thickness after forming, billets with greater thickness have better formability of sheets under embossing process because there

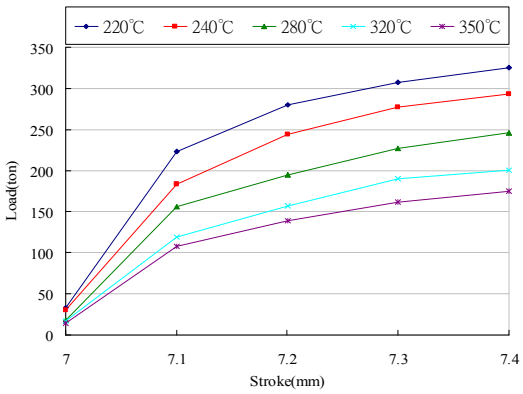

Fig. 4 Simulation results for punch load and stroke under different formation temperatures

are more materials for filling the space of cavities, and the load during forming is also obviously reduced. If the thickness of billets is thinner, the materials for filling the space of cavities would be less, and the required forming load will be relatively increased, as shown in Fig. 5. However, billets with smaller thickness produce smaller area of spill edge and less material waste, as shown in Fig. 6. Currently, lightweight and small-sized 3C products with thin shells are more popular, leading to the trend of production of thinner products. Therefore, under the prerequisites of no effect on product strength, decrease of spill edge and tolerable forming load of forging machine, the study selects the magnesium sheet with billet thickness 2.1 mm as the material for carrying out subsequent simulation analysis and hot forging experiment.

The paper explores the effects of billet dimensions on the formability of sheets under embossing process. During simulation for analysis, let the billet thickness be 2.1 mm, and the dimensions of 3 kinds of billets be 93 mm × 63 mm, 90 mm × 60 mm and 87 mm × 57 mm respectively. As known from the results of simulation analysis, the dimensions of billets have very great effects on the formability of sheets under embossing process. Billets with greater area have better formability of sheets under embossing process. However, the action force required for forming is also relatively greater, as shown in Fig. 7. Nevertheless, when the dimensions o billets are certain fixed values, there would be insufficient materials for fully filling the space of cavities, leading to production of defects on finished products and creating quality problems on the surface.

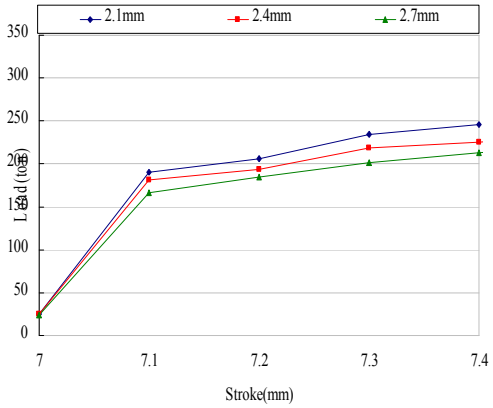

Fig. 5 Simulation results for punch load given billets of different thicknesses

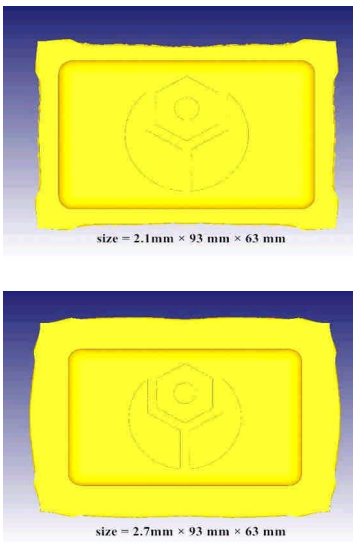

Fig. 6 Spilled edge area acquired via simulation using billets of different thicknesses

First of all, preset the simulation parameters for cavities filling of billets, including heating temperature 280℃, punching speed 0.9 mm/s, constant shear friction factor 0.18, height 1mm of embossing style, final stroke distance 7.4 mm, and spill edge thickness 1. 2 mm. When the punch moves downwards at stroke 7.0 mm, the sheet is attached with force and bends, and gradually touches the bottom area of the mother die, as shown in Fig. 8(a), forcing part of the billets to gradually get close to the cavities of the embossing pattern between the punch and the mother die,

and making the material unable to flow towards the gaps by the two sides. The material around the cavities slowly changes its flowing direction, so the material can only move into the cavities. When the stroke continues to increase to 7.3 mm, the upward flowing speed of the material inside the cavities of the embossing pattern is greater than the downward flowing speed of the material towards the two sides, making the space of cavities being continuously filled, as shown in Fig. 8(b). When the punch moves downwards at stroke 7.4 mm, the space of cavities has been fully filled. The excessive material can only move to the two sides to form spill edge. This phenomenon also leads to the trend that the forming load finally rises, as shown in Fig. 8(c). Since the embossing pattern in the middle of sheet is under extrusion by the upper and lower dies, the stress and strain values are obviously greater. And at the sharp parts of the embossing pattern, since the material has to squeeze into the sharp angles of the die, the values of the produced stress and strain are obviously greater than those of other embossing patterns.

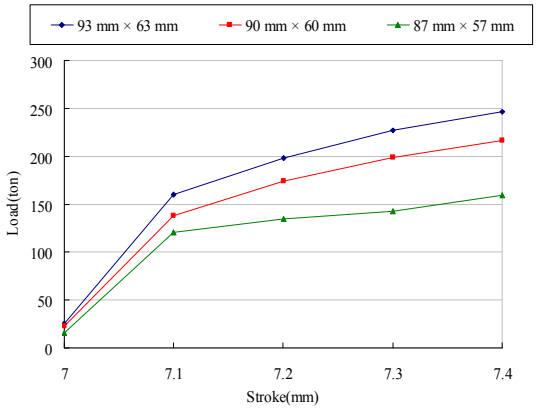

Fig. 7 Simulated punch load given billets with different dimensions

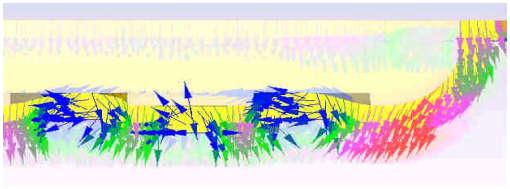

(a) stroke =7.0mm

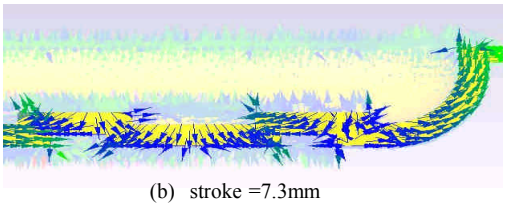

(b) stroke =7.3mm

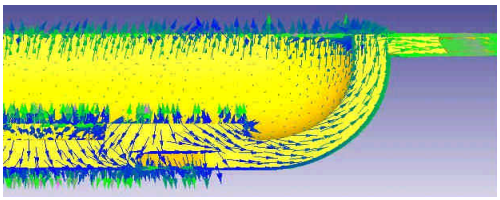

(c) stroke =7.4mm

Fig. 8 Material flow when the punch is depressed at different strokes before cavity filling

Fig. 9 is the schematic diagram of the expected finished product under embossing process. The dimensions of the finished product under embossing process are compared with those of the simulation results after cavities are fully filled, as shown in Fig. 10. As known from the figure, the dimensions of a hexagon and a circle appeared in the embossing pattern of the actual finished product are 19.84 mm and 7.96 mm respectively, and the simulation results are 19.58 mm and 8.02 mm respectively. When spill edge is not considered, the dimensions of the actual finished product under embossing process are not consistent with those of the finished product obtained from simulation. Thus, it can be found that the simulation analysis model developed by the study can correctly analyze the flowing way of metallic materials. As known from the experiment, when the forming temperature is above 220℃, all kinds of embossing patterns can be formed completely, and the forming load tends to decrease with the rise of forming temperature. A comparison of sectional dimensions between the experimental finished product under embossing process and the finished product obtained from simulation is shown in Fig. 11. As known from the figure, the round angle of the experimental finished product and the central part of the sheet are in dimensions 1.74 mm and 1.75 mm respectively, and the simulation results are 1.72 mm and 1.69 mm respectively. The experimental finished product has embossing pattern at the height 1.03 mm, and the simulation result is 0.98 mm. As known from the analysis, the experimental and simulative finished products have consistent sectional dimensions. Therefore, it is known that the simulation analysis software can correctly simulate the filling situation of cavities by material. In the embossing experiment undergone by the study, graphite lubricant is used. As graphite possesses excellent lubrication effect under high temperature, it is suitable for application to high-temperature forging of magnesium alloy. Nevertheless, in a real embossing experiment, it is required to decrease the accumulated residues on the surface of die; otherwise, excessive residue would make the embossing pattern have rough and uneven surface. Therefore, before embossing experiment is carried out, sediments should be firstly removed from the surface of die, which should then be evenly coated with lubricant. By doing so, the surface of the finished product would be smooth, and would not cause defect to the surface of the embossing pattern. As to the forming load, at 220℃ the experimental load is 330.07 tons, and the simulative load is 325.70 tons, with a difference of 4.37 tons in between, and an error of about 1.34%. At 280℃ the experimental load is 256.44 tons, and the simulative load is 246.32 tons, with a difference of 10.12 tons in between, and an error of about 4.10%. At 350℃ the experimental load is 187.10 tons, and the simulative load is 174.65 tons, with a difference of 12.45 tons in between, and an error of about 7.12%. As known from Fig. 12, the forming loads in both the experiment and simulation tend to have linear decline with the rise of forming temperature.

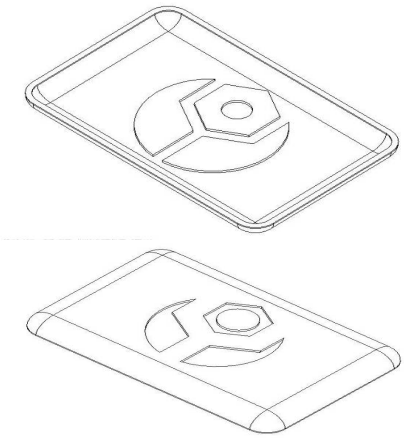

Fig. 9 Schematic diagram of the finished product under embossing process

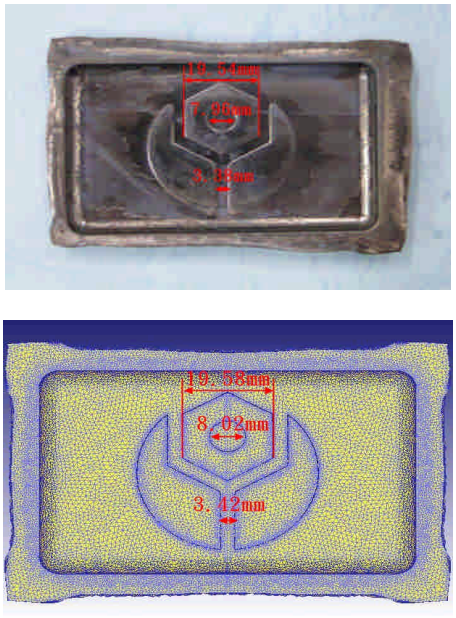

Fig. 10 Comparison between the finished product under the embossing process and the simulation result

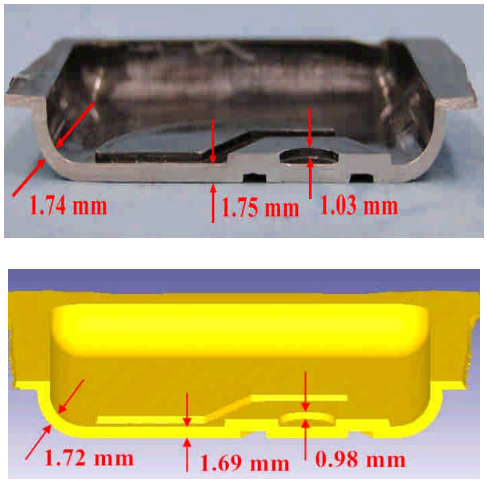

Fig. 11 Cross-section of finished products obtained from the experiment and the simulation

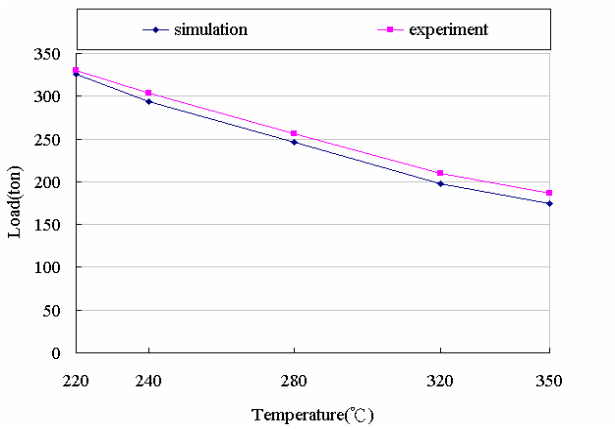

Fig. 12 Comparison of loads obtained via the experiment and simulative forming

The position for hardness observation of sheet under embossing process is shown in Fig. 13, with measurement results shown in Table 2. In the forging process, graphite is taken as lubricant. Under the same friction conditions, if the forging temperatures of billets are different, the obtained conclusions are: for hot forging at 220℃, since the forming temperature is lower, the material fluidity is poor. This is because under the softening effects caused by high temperature, higher forming temperature makes the hardness value of finished products become lower. Among the embossing patterns, hexagon pattern has greater plastic deformation and greater strain value, so its hardness value is greater than other patterns.

The observation position of the metallography of sheets under embossing process is shown in Fig. 13. Fig. 14 shows the microstructure of the graphite-lubricant-added magnesium alloy sheets under embossing process at forming temperature 320℃. As known from the experimental results, under the same friction conditions, when forming temperature is higher, the grains of the material of magnesium alloy sheets after forging would be greater, and the hardness of the finished product would be reduced. Besides, the grain structure at the embossing pattern (position A) is finer than that on the slab at the bottom of sheet (position B).

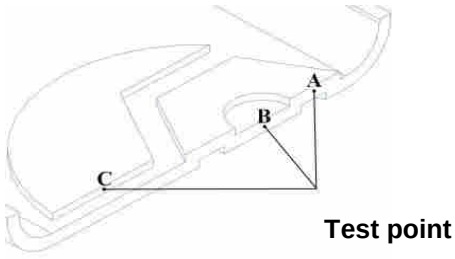

Fig. 13 Observation position of sheet hardness under embossing

TABLE 2 Hardness of finished products forged under different temperatures

POSI. / HARD. / TEMP.	A	B	C
220℃	63.9	63.4	62.7
280℃	60.3	59.9	58.8
320℃	55.7	55.4	55.1

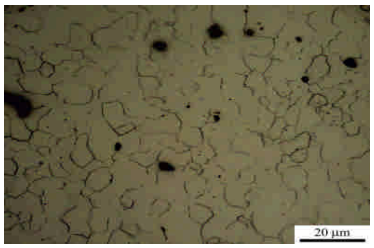

(a) A

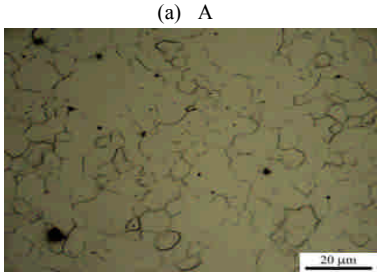

(b) B

Fig. 14 Microstructure of metallography following forging at forging temperature 320℃

IV. Conclusions

The paper mainly explores AZ31 magnesium alloy sheets under embossing process. First of all, the finite element analysis software, DEFORM is used to carry out simulation analysis so as to explore the effects of taper bevel angle of die, round corner radius of die, dimensions of billets, thickness of billets, constant shear friction factor, punching speed and forming temperature on the formability of embossing patterns, and also to know the load, stress and strain distribution in the forming of sheets under embossing process. Secondly, an experiment of magnesium alloy sheets under embossing process is carried out for observation of the change of embossing pattern and forming load under different forming temperatures. Finally, through hardness test and observation of metallography, the paper assesses the effects of embossing process under different temperatures on the strength and microstructure of finished products. After collation and analysis, the following conclusions are drawn:

1. As shown from the analytic results of simulation of magnesium alloy sheets under embossing process, the round corner radius of die is 0.3 mm, and when the taper bevel angle of die is $\alpha = 3^{\circ}$, the shape of embossing pattern is the best, and the forming load is lowest.
2. When forming temperature is higher and constant shear friction factor is lower, the forming load tends to reduce. Besides, an increase of moving speed of punch has smaller effects on forming load. After simulation analysis and making comparison with experimental results, the simulative model used by this paper can give considerable accuracy in the prediction of forming load and the prediction of shape after forming.
3. As shown from the experimental results of magnesium alloy sheets under embossing process, excessive residue of graphite lubricant on the surface of die would form rough and uneven surface on finished products. Therefore, before forming, the residue of lubricant accumulated on the surface of die has to be removed.

Acknowledgment

The authors would like to thank the National Science Council of the Republic of China, Taiwan for financially supporting this research under Contract No. NSC98-2221-E-149-002.

REFERENCES

1. R. Ye. Lapovok, M. R. Barnett and C. H.J. Davies, Construction of extrusion limit diagram for AZ31 magnesium alloy by FE simulation, *Journal of Materials Processing Technology*, Vol. 146 (2004), 408-414.
2. L. Li, J. Zhou and J. Duszczyk, Determination of a constitutive relationship for AZ31B magnesium alloy and validation through comparison between simulation and real extrusion, *Journal of Materials Processing Technology*, Vol. 172 (2006), 372-380.
3. Fuh-Kuo Chen and Jia-Wen Tsai, A study of size effect in micro-forming with micro-hardness tests, *Journal of Materials Processing Technology*, Vol. 177 (2006), 372-380.
4. Hu Yamin, Lai Zhouyi and Zhang Yucheng, The study of cup-rod combined extrusion process of magnesium alloy (AZ61A), *Journal of Materials Processing Technology*, Vol. 187-188 (2007), 649-652.
5. Sutasn Thipprakmas, Masahiko Jin and Masao Murakawa, Study on flanged shapes in fineblanked-hole flanging process(FB-hole flanging process) using finite element method (FEM), *Journal of Materials Processing Technology*, Vol. 192-193 (2007), 128-133.
6. K. Mueller and S. Muller, Severe plastic deformation of the magnesium alloy AZ31, *Journal of Materials Processing Technology*, Vol. 187-188 (2007), 775-779.
7. G. Liu, J. zhou and J. Duszczyk, Prediction and verification of evolution as a function of ram speed during the extrusion of AZ31 alloy into a rectangular section, *Journal of Materials Processing Technology*, Vol. 186 (2007), 191-199.
8. Heng-Kuang Tsai, Chien-Chin Liao and Fuh-Kuo Chen, Die design for stamping a notebook case with magnesium alloy sheets, *Journal of Materials Processing Technology*, Vol. 201 (2008), 247-251.